Neoplasia • Vol. 9, No. 2, February 2007, pp. 136–146 136

www.neoplasia.com

Genes and Proteins Differentially Expressed during *In Vitro* Malignant Transformation of Bovine Pancreatic Duct Cells[1]

R. Jesnowski, Dmitri Zubakov†, Ralf Faissner*, Jörg Ringel*, Jörg D. Hoheisel†, Ralf Lösel‡, Martina Schnölzer§ and Matthias Löhr**

*Clinical Cooperation Unit Molecular Gastroenterology (E180), German Cancer Research Center Heidelberg and Department of Medicine II, Medical Faculty of Mannheim, University of Heidelberg, Heidelberg, Germany; †Functional Genome Analysis (B070), German Cancer Research Center Heidelberg, Heidelberg, Germany; ‡Institute for Clinical Pharmacology, Medical Faculty of Mannheim, University of Heidelberg, Heidelberg, Germany; §Protein Analysis Facility (B100), German Cancer Research Center Heidelberg, Heidelberg, Germany

Abstract

Pancreatic carcinoma has an extremely bad prognosis due to lack of early diagnostic markers and lack of effective therapeutic strategies. Recently, we have established an *in vitro* model recapitulating the first steps in the carcinogenesis of the pancreas. SV40 large T antigen–immortalized bovine pancreatic duct cells formed intrapancreatic adenocarcinoma tumors on *k-ras*^{mut} transfection after orthotopic injection in the nude mouse pancreas. Here we identified genes and proteins differentially expressed in the course of malignant transformation using reciprocal suppression subtractive hybridization and 2D gel electrophoresis and mass spectrometry, respectively. We identified 34 differentially expressed genes, expressed sequence tags, and 15 unique proteins. Differential expression was verified for some of the genes or proteins in samples from pancreatic carcinoma. Among these genes and proteins, the majority had already been described either to be influenced by a mutated *ras* or to be differentially expressed in pancreatic adenocarcinoma, thus proving the feasibility of our model. Other genes and proteins (e.g., *BBC1*, *GLTSCR2*, and *rhoGDIα*), up to now, have not been implicated in pancreatic tumor development. Thus, we were able to establish an *in vitro* model of pancreatic carcinogenesis, which enabled us to identify genes and proteins differentially expressed during the early steps of malignant transformation.

Neoplasia (2007) **9,** 136–146

Keywords: Transcriptomics, proteomics, ki-ras, SV40 large T, pancreatic carcinogenesis.

Introduction

Pancreatic cancer is the fourth most common cause of cancer deaths [1]. Its incidence is increasing, affecting about 10 per 100,000 population per year in western countries. Because no screening markers are available up to now and due to lack of early symptoms, the majority of tumors are already in advanced nonresectable stages at the time of diagnosis, and no therapeutic strategy developed so far has resulted in a considerable increase in long-term survival. This is why the prognosis of this disease is still very dismal, with 5-year survival rates of < 5% [2]. An important approach to the understanding of the biology and molecular alterations involved in the carcinogenesis of this disease is the development of relevant *in vitro* and *in vivo* models. These models may provide new diagnostic tools that would allow diagnosis at earlier stages, and this in turn may result in an increase in long-term survival. Because most pancreatic tumors are of ductal phenotype [3] and may derive from ductal epithelial cells [4], the cultivation of isolated human pancreatic duct epithelial cells may play a crucial role in the development of an *in vitro* model for pancreatic carcinogenesis.

In recent years, numerous alterations associated with carcinogenesis have been identified, namely, mutation of the *ki-ras* oncogene. More than 90% of pancreatic adenocarcinomas harbor mutations of this gene; these mutations are detectable as well in early stages of tumor development (PanIN lesions) [5], as in metastatic tumors. Thus, mutation of the *ki-ras* oncogene seems to be an early and important event in the tumorigenesis of the pancreas.

Recently, we were able to establish an *in vitro* model by mimicking the first steps of the carcinogenesis of the pancreas. We immortalized bovine pancreatic duct cells through transfection with SV40 large T antigen. These immortal cells were then transfected additionally with a vector coding for a mutated *ki-ras* gene (codon 12: GGT→GTT). Both cell lines were characterized in detail and showed classic markers of differentiated pancreatic duct cells [carbonic anhydrase type II, cytokeratins (CK) 7 and 19, and others], but they exhibited

Address all correspondence to: R. Jesenofsky (R. Jesnowski), Clinical Cooperation Unit Molecular Gastroenterology (E180), German Cancer Research Center, Im Neuenheimer Feld 581, Heidelberg D-69120, Germany. E-mail: r.jesenofsky@dkfz.de

[1]This article refers to supplementary material, which is designated by "W" (i.e., Table W1) and is available online at www.bcdecker.com.

Received 22 November 2006; Revised 15 January 2007; Accepted 16 January 2007.

DOI 10.1593/neo.06754

marked differences in their tumorigenic potential. Although the only immortalized cell line was neither able to grow in soft agar nor able to induce tumor, mutated *ki-ras*–expressing cells grew in soft agar and formed tumors and liver metastases when inoculated orthotopically in the pancreas of nude mice [6]. In an attempt to characterize the transition from an almost benign cell lineage to an invasive ductal adenocarcinoma, we asked for changes in gene expression at both RNA and protein levels. Here we describe the analysis and identification of genes and proteins that are differentially expressed during this course of malignant transformation.

Materials and Methods

RNA Isolation

Total RNA was prepared from pancreatic tissue samples, using the ToTally RNA kit (Ambion, Inc., Austin, TX), according to the protocol supplied by the manufacturer. RNA from pancreatic cell lines VA and VAras^{mut} was isolated with RNeasy mini kit (Qiagen, Inc., Hilden, Germany) following the manufacturer's recommendations. For suppression subtractive hybridization (SSH) analysis, total RNA was treated with Dnase I (Ambion, Inc.) to remove traces of genomic DNA. Poly A$^+$ RNA was isolated from total RNA preparations using oligo(dT)-conjugated magnetic Dynabeads (Dynal Biotech, Oslo, Norway).

SSH

SSH was performed using the PCR-Select cDNA Subtraction Kit (BD Clontech, Heidelberg, Germany). VAras^{mut} and VA RNA isolations were reciprocally compared by forward and reverse subtractions. Driver and tester cDNA were produced, each from 2 μg of Poly A$^+$ RNA, following the manufacturer's guidelines. Synthesized cDNA were digested with the restriction enzyme *Rsa*I, and tester cDNA populations were divided into two tubes and ligated to adaptor 1 or adaptor 2R. Subtractive hybridization was performed by adding 1.5 μl of driver cDNA to each tube, one containing 1.5 μl of adaptor 1 and the other containing 1.5 μl of adapter 2R–ligated diluted tester cDNA in 1 μl of 4× hybridization buffer. After denaturation, samples were allowed to anneal at 68°C for 8 hours. Following the first hybridization, the two samples were combined simultaneously with the addition of 1 μl of freshly denatured driver cDNA, and hybridization was continued overnight at 68°C. Products from the second hybridization were diluted in 200 μl of dilution buffer (20 mM HEPES pH 8.3, 50 mM NaCl, and 0.2 mM EDTA), heated at 68°C for an additional 7 minutes, and stored at −20°C.

Polymerase Chain Reaction (PCR) Amplification of Subtracted Products

PTC-200 Thermal Cycler (MJ Research, Waltham, MA) was used to perform PCR amplification of subtracted tester products. Primary PCR amplifications were conducted for each tester using diluted subtracted products following the second hybridization. One microliter of sample was added to 24 μl of PCR master mix prepared using the reagents supplied in the kit, and cycling conditions commenced as follows: 75°C for 5 minutes to extend the adaptors; 94°C for 25 seconds; and 27 cycles at 94°C for 10 seconds, 66°C for 30 seconds, and 72°C for 1.5 minutes. Amplified products were diluted 10-fold in sterile water, and 1 μl of diluted primary PCR products was added to 24 μl of secondary PCR master mix containing nested primers (1 and 2R) to ensure the specific amplification of double-stranded templates containing both adaptors. Secondary PCR was performed at 94°C for 10 seconds, 68°C for 30 seconds, and 72°C for 1.5 minutes (cycle numbers were 18 and 19 for VAras^{mut} and VA, respectively). PCR products were analyzed on a 2% agarose gel.

Cloning of Subtracted cDNA Templates

Following secondary PCR amplification, subtracted products from each tester cDNA population were purified using the QIAquick PCR Purification Kit (Qiagen, Inc.). Thus, short DNA fragments below 100 bp were removed before cloning. Purified products were ligated with the pGEM T-Easy vector (Promega Corp., Madison, WI) and used for the electrotransformation of competent DH5α *Escherichia coli* cells. Colonies were grown in a selective LB agar medium containing X-gal and isopropyl β-D-1-thiogalactopyranoside (IPTG) for the screening of blue/white colony. For each tester, 384 colonies were randomly picked up in microtiter plates and grown overnight in a liquid LB medium.

Differential Screening By Microarray Hybridization

To confirm the unique expression of subtracted products, all cDNA clones were subjected to differential screening by microarray hybridization. First, inserts from 768 selected clones (384 clones for each tester) were PCR-amplified with T7 and SP6 primers. PCR was performed by adding 0.5 μl of saturated growth liquid culture to 100-μl PCRs containing 10 mM Tris (pH 9.0), 50 mM KCl, 150 μM dNTP, 3 M betaine, 30 mM cresol red, and 2.0 U of *Taq* DNA polymerase (MBI Fermentas, St. Leon-Rot, Germany) in 96-well plates. Thermal cycling conditions consisted of initial denaturation at 95°C for 3 minutes, followed by 35 cycles of denaturation at 95°C for 30 seconds, annealing at 53°C for 30 seconds, and elongation at 72°C for 3 minutes, with a final 10-minute extension at 72°C in PTC-200 Thermal Cycler (MJ Research). Five microliters of each PCR was examined on a 2% agarose gel. PCR fragments were purified by isopropanol precipitation.

SSH products from both subtraction experiments were combined on a slide. Quadruplicate spotting onto a custom-made poly-L-lysine surface was carried out with SDDC-2 DNA Microarrayer (Engineering Services, Inc., Toronto, Canada), using betaine spotting solution, according to the protocol described previously [7]. Poly A$^+$ RNA isolated from VAras^{mut} and VA cells (0.5 μg each) was labeled by direct incorporation of either Cy3 or Cy5 fluorescent dye using SuperScript II reverse transcriptase (Invitrogen, Inc., Karlsruhe, Germany) and oligo-d(T)$_{20}$ as a primer. Labeled probes were purified through QIAquick PCR purification columns (Qiagen, Inc.), dried in a SpeedVac (Qiagen, Inc.), and resuspended in a total volume of 16 μl of hybridization buffer [3× SSC (0.45 M NaCl, 0.045 M sodium citrate), 1% sodium dodecyl sulfate

(SDS), 5× Denhardt's solution, 100 mg/ml sheared salmon sperm DNA, 50% formamide, and 10% dextran sulfate]. The probes were denatured at 80°C for 10 minutes and applied to arrayed/denatured slides at 45°C for 16 hours in a humidified chamber (Telechem, Inc., Sunnyvale, CA). Hybridized slides were washed in 2× SSC and 0.1% SDS for 5 minutes at room temperature and in 0.2× SSC for 5 minutes before scanning by the ScanArray 5000 Microarray Analysis System (GSI Lumonics, Inc., Watertown, MA).

Separate images with 10-μm resolution were captured for each of two fluorophores used. GenePix v. 4.0 (Axon Instruments, Inc., Union City, CA) software was used to quantitate signals at each spot. Signal intensity filtering and background signal correction for spots were performed using GP3 perl script (http://www.bch.msu.edu/~zacharet/microarray/gp3.html) [8].

Feature spot signals were normalized relative to signals from external controls: *Arabidopsis thaliana* genes spotted on arrays together with SSH PCR products (the corresponding *Arabidopsis* mRNA was spiked into labeling reactions in known concentrations).

The mean ratios of Cy3 and Cy5 signal intensities for individual spots were calculated by averaging the data obtained in four independent hybridizations with ''dye flip.'' Genes were considered differentially expressed when all hybridizations showed a > 2-fold change. The sequencing of PCR products was performed at Genotype, Inc. (Hirschhorn, Germany), a company providing commercial DNA analysis service.

Homology searches were performed using the Basic Local Alignment Search Tool (BLAST) on the combined GenBank/EMBL nonredundant (nr), expressed sequence tag (EST), and SwissProt databases (National Center for Biotechnology Information, which can be accessed online at www.ncbi.nlm.nih.gov).

Two-Dimensional Gel Electrophoresis

Protein extraction from cells obtained from different passages was performed with 1 ml of lysis buffer (9.5 M urea, 2% 3-[(3-Cholamidopropyl)dimethylammonio]-1-propanesulfonate (CHAPS), 0.8% Pharmalyte 3-10, 1% dithiothreitol (DTT), and 5 mM Pefabloc SC PLUS; Roche Diagnostics, Inc., Mannheim, Germany). After centrifugation at 13,000*g* at 15°C for 60 minutes, the protein solution was collected and stored at −80°C until use. Protein concentration was determined by the Bio-Rad Protein Assay (Bio-Rad, Munich, Germany), using a UV/Visible spectrophotometer (Utrospec 2000; Pharmacia Biotech, Uppsala, Sweden).

Samples (protein concentration, ~ 1–3 μg/μl) were loaded into linear immobilized gradient (IPG) strips (Immobiline DryStrips, pH 4–7; Amersham Biosciences, Freiburg, Germany) using 50 μg of total protein per strip. The IPG strips were rehydrated (10 hours, 30 V, and 20°C) in a solution (350 μl) of 8 M urea, 2% CHAPS, 0.5% IPG buffer pH 4–7, 16 mM DTT, and a calculated amount of protein sample. Separation in the first dimension was performed on an IPGphor unit (Amersham Biosciences). The IPG strips were focused for a total of 125 kV hour. Before the second dimension separation, the IPG strips were equilibrated in equilibration buffer twice for 20 minutes (50 mM Tris–HCl pH 8.8, 6 M urea, 30% glycerol, and 2% SDS) containing DTT (10 mg/ml) and iodoacetamide (40 mg/ml), respectively.

The second dimension [SDS polyacrylamide gel electrophoresis (PAGE)] was performed on laboratory-made polyacrylamide gels (12.5% T; 1.5 × 200 × 250 mm) running on a vertical Hoefer DALT Electrophoresis Tank (Amersham Biosciences). Electrophoresis was carried out for about 22 hours in TGS electrode buffer (25 mM Tris, 192 mM glycine, and 0.1% SDS pH 8.3) at 10°C, applying a constant voltage of 85 V.

Gel Analysis

2-DE separated protein spots were visualized with a modified silver-staining method compatible with matrix-assisted laser desorption/ionisation–time of flight–mass spectrometry (MALDI-TOF-MS) [9]. Silver-stained gels were digitized using a GS-800 densitometer (Bio-Rad), and images were imported in a 2D gel image analysis program on a set of six gels per sample. PDQuest 7.1 (Bio-Rad) was used to locate and quantify protein spots and to match spots through the gels. The quantity of each protein spot was normalized against the total quantity arising from all valid protein spots on the gel. Statistical comparison between individual protein abundances was conducted by the calculation of Student's *t* test within the PDQuest analysis, with a significance level of at least 90%.

Protein Identification By MALDI-MS

Gel pieces containing proteins of interest were manually excised and subjected to in-gel digestion. Proteins were reduced, alkylated, and digested with sequencing-grade modified trypsin (Promega Corp.) using 10 μl of trypsin (10 ng/μl in 40 mM NH_4HCO_3). Tryptic digested MALDI samples were prepared by cocrystallization of a saturated solution of the matrix (α-cyano-4-hydroxycinnamic acid in 50/50 vol/wt.% acetonitrile/0.1% trifluoroacetic acid in water) with $ZipTip_{C18}$ (Millipore, Inc., Schwalbach, Germany) concentrated samples.

MALDI mass fingerprint spectra were recorded in positive ion mode with delayed extraction with a Reflex II TOF instrument (Bruker Daltonics, Inc., Bremen, Germany). Calibration was performed internally by a two-point linear fit using the autolysis products of trypsin at m/z = 1045.56 and m/z = 2211.10. Tryptic monoisotopic peptide masses were searched against NCBInr and SwissProt databases using the Mascot (Matrix Science, Ltd., London, Great Britain) and ProFound (Rockefeller University, New York, NY) programs.

Verification of Differential Gene and Protein Expression in Chronic Pancreatitis and Pancreatic Adenocarcinoma

To verify that the differential gene expression identified in our model system holds true *in vivo*, the expression of selected genes was analyzed in samples from normal pancreas, chronic pancreatitis, and pancreatic adenocarcinoma, using semiquantitative reverse transcription (RT) PCR.

Intron spanning primers for the respective genes (Table 1) were designed, using the online software Primer3 (www.broad.mit.edu/cgi-bin/primer/primer3_www.cgi), to identify possible genomic DNA contamination. To ensure that the PCR was in its logarithmic phase, the appropriate cycle number for each single gene was determined in prior experiments. PCR conditions were as follows: 94°C for 15 minutes, cycling at 94°C for 45 seconds, 60°C for 45 seconds, and 72°C for 1 minute, followed at the end by an extension step at 72°C for 10 minutes.

The differential protein expression of annexin 1 was analyzed by immunohistochemistry in paraffin-embedded tissue samples obtained from resections due to chronic pancreatitis and pancreatic carcinoma using standard protocols. In brief, tissue sections were deparaffinized in xylene (2 × 5 minutes), rehydrated in a graded series of ethanol, blocked with 10% fetal calf serum, and incubated for 45 minutes with anti–annexin 1 antibody [1:100 in phosphate-buffered saline (PBS)–bovine serum albumin (BSA); Santa Cruz Biotechnology, Santa Cruz, CA]. After incubation with the second antibody (rabbit–anti-mouse HRP, 1:100, in PBS–BSA; Dako, Inc., Hamburg, Germany), slides were developed using AEC substrate (Chemicon, Hampshire, Great Britain).

Results

Genes Differentially Expressed in ras-Transformed Pancreatic Duct Epithelial Cells

The secondary SSH PCR resulted in a distinct banding pattern and low background. Cloned subtraction SSH products were PCR-amplified and robotically spotted on microarrays along with normalization control DNA. The microarrays were hybridized with Cy5/Cy3–labeled RNA isolated from VAras^{mut} and VA cells. After statistical analysis of hybridization results, 65 clones were considered differentially expressed and sequenced. Among these, 28 unique genes and 6 ESTs were identified; 16 of them were upregulated and 18 were downregulated in VAras^{mut} cells. The results of the BLAST homology search are presented in Table 2. Of the 28 annotated genes, 14 already had been described to be either influenced by a mutated *ras* or differentially expressed in pancreatic adenocarcinoma (Table 2), thus proving the validity of our model. Other genes (e.g., *epsin 1*, *apolipoprotein A1*), up to now, have not been implicated in ras signaling. Most of the upregulated genes accounted for proteins of the cytoskeleton-like 40-kDa keratin, CK7, CK18, CK19, and myosin regulatory light chain. Moreover, several extracellular matrix proteins, as Col Iα1, Col Vα2, and osteonectin/SPARC, were upregulated. Additionally, two ribosomal proteins (mRPS34 and RPL26) and α enolase were upregulated. In contrast, the downregulated genes composed a rather heterogeneous group. Thus, three ribosomal proteins (RPS5, RPS19, and RPL39) and two putative tumor-suppressor genes, breast basic conserved 1 (*BBC1*) and *GLTSCR2*, were downregulated. Additionally, two genes involved in tumor immunology/tumor rejection, major histocompatibility complex (MHC) class 1 protein molecule D18.3 and *SCART1*, were downregulated. For the remaining downregulated genes (Table 2), no grouping concerning functional criteria was possible.

Table 1. Primers Used for the RT-PCR of Human Tissue Samples.

Gene Name	Primer Sequence	Product Size (bp)
Annexin 1	Forward: 5′-ATGTCGCTGCCTTGCATAA Reverse: 5′-CCTCAGATCGGTCACCCTTA	432
BBC1	Forward: 5′-GTTCGGTACCACACGAAGGT Reverse: 5′-ACTGCCGACTGATTCCAAGT	480
rhoGDIα	Forward: 5′-TTTCCGCAGACCCCAAC Reverse: 5′-GAGATTCCACTCCCAGGACA	406
SCART1	Forward: 5′-TACAGCAGCTGCGAGACAGT Reverse: 5′-TCCTCATCCCGTTCAAAGTC	222

Proteins Regulated By Activated ras in Pancreatic Duct Cells (PDCs)

Identification of proteins from 2D gels of VA and VAras^{mut} cell lysates obtained from four independent experiments was conducted by MALDI mass fingerprinting. At the protein level, 36 protein spots were identified by mass spectrometry, representing 22 unique proteins (Table W1 and Figure 1). For several proteins [heat shock protein (HSP) 70, actin, vimentin, CK8, and CK19], different isoforms or fragmented proteins (CK8 and tubulin) were identified. Of the 36 analyzed protein spots, 11 were found to be upregulated and 9 were found to be downregulated in the majority of experiments by at least 1.5-fold in VAras^{mut} cells (Table 3), whereas for the remainder, the expression was unchanged or expression changes were inconsistent. These 20 differentially expressed protein spots represented 15 unique proteins. Also at the protein level, several proteins (β actin, annexin 1, CK8, HSP70, myosin regulatory light chain, and vimentin) already had been demonstrated to be differentially expressed in pancreatic adenocarcinoma, again proving the validity of our model. Additionally, tropomyosin 1, fragmented α tubulin, γ actin, and proliferating cell nuclear antigen (PCNA) were found to be downregulated, whereas stress-induced phosphoprotein 1, HSP27, Grp58, rho guanine dinucleotide phosphate dissociation inhibitor α (*rhoGDIα*), and fragmented β tubulin were upregulated in VAras^{mut} cells.

Verification of Differential Gene and Protein Expression in Chronic Pancreatitis and Pancreatic Adenocarcinoma

We attempted to verify the differential gene expression identified in our model system *in vivo*; thus, the expression of selected genes and proteins was analyzed in samples from normal pancreas, chronic pancreatitis, and pancreatic adenocarcinoma using semiquantitative RT-PCR or immunohistochemistry. We concentrated our expression analysis on genes, which up to now have not been reported to be differentially expressed in pancreatic adenocarcinoma. However, annexin 1, known for being overexpressed in pancreatic cancer, was included. For the putative tumor-suppressor *BBC1*, we were able to verify the downregulation observed in VAras^{mut} cells in samples of pancreatic cancer (Figure 2, *upper panel*). Moreover, also for the gene *rhoGDIα*, which

Table 2. Putative Homology and Identities of cDNA Differentially Expressed in VAras^{mut} Cells.

Number	Expression Change	Homology	Base Pairs Submitted to BLAST	GenBank Accession Number	Identities
Upregulated					
1	*	Collagen, type I, α 1	534	NM_000088	Human 290/309 (93%)
2	*	CK19 gene	454	X04198	Bovine 149/151 (98%)
3	*	Keratin 7	320	BC002700	Human 135/146 (92%)
4	*	Osteonectin	451	J03233	Bovine 194/195 (99%)
5	†	40-kDa keratin intermediate filament precursor gene	429	J03607	Human 188/204 (92%)
6	†	Keratin 18	365	NM_000224	Human 154/176 (87%)
7	†	Myosin regulatory light chain	377	D82057	Human 173/185 (93%)
8	‡	α Enolase mRNA	433	AF149256	Bovine 193/201 (96%)
9	‡	Clathrin heavy chain	549	U31757	Bovine 283/285 (99%)
10	‡	EST	336	CB446148	Bovine 207/237 (87%)
11	‡	EST	360	CB464940	Bovine 180/196 (91%)
12	‡	Hypothetical protein MGC10731	540	NM_030907	Human 161/185 (87%)
13	‡	Hypothetical protein MGC2963	700	NM_031298	Human 331/359 (92%)
14	‡	Mitochondrial ribosomal protein S34	560	NM_023936	Human 312/365 (85%)
15	‡	Procollagen, type V, α 2	458	XM_193986	Mouse 107/125 (85%)
16	‡	Ribosomal protein L26	372	AB093679	Primate 112/137 (81%)
Downregulated					
1	*	Breast basic conserved 1	433	AF192977	Ovine 184/190 (96%)
2	*	Ezrin	576	M98498	Bovine 414/415 (99%)
3	*	MHC class 1 protein molecule D18.3	463	Y09207	Bovine 266/266 (100%)
4	*	Proliferating cell nuclear antigen	550	AF416380	Ovine 304/318 (95%)
5	*	Ribosomal protein S5	686	BC018828	Human 275/324 (84%)
6	†	ADP/ATP translocase T2	367	M24103	Bovine 159/160 (99%)
7	†	Apolipoprotein A-I	520	M35870	Bovine 316/322 (98%)
8	†	β Actin	469	AF129289	Ovine 175/186 (94%)
9	†	Chromosome 21 open reading frame 59 (C21orf59)	664	NM_021254	Human 433/494 (87%)
10	†	Epsin 1	577	NM_057136	Rat 461/515 (89%)
11	†	EST	272	BM433009	Bovine 134/142 (94%)
12	†	Glioma-tumor-suppressor candidate region gene 2	413	BC013307	Human 199/235 (84%)
13	†	Ribosomal protein L30	277	AF063243	Bovine 112/113 (99%)
14	†	Squamous cell carcinoma antigen recognized by T cells 1	537	BC028823	Mouse 264/310 (85%)
15	‡	EST	443	AV609800	Bovine 226/228 (99%)
16	‡	EST	575	BE751110	Bovine 469/475 (98%)
17	‡	EST	523	CB462154	Bovine 309/324 (95%)
18	‡	Ribosomal protein S19	324	BC018616	Human 145/153 (94%)

*Expression change, > 5-fold.
†Expression change, > 3-fold.
‡Expression change, > 2-fold.

is overexpressed in VAras^{mut} cells, a trend for an overexpression in samples of pancreatic adenocarcinoma was detectable (Figure 2, *lower panel*). In contrast, the expression of the gene squamous cell carcinoma antigen recognized by T cells (*SCART1*), which was downregulated in VAras^{mut} cells, was not changed in pancreatic adenocarcinoma (Figure 2, *middle panel*).

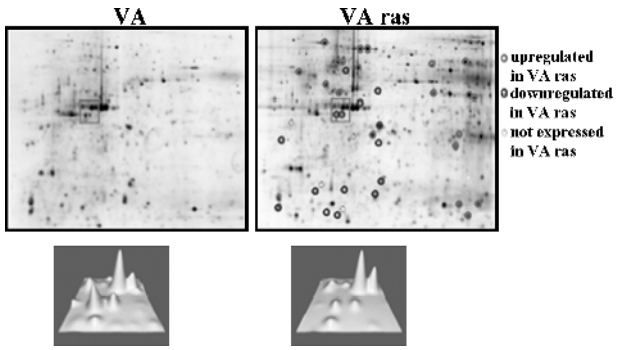

Figure 1. *Two-dimensional gel electrophoresis of VA and VAras^{mut} cell lysates. Differentially expressed proteins are marked by circles. In the rectangles in the lower panel, the intensities of the respective spots are illustrated in 3D; the region shown corresponds to the rectangles in the upper panel.*

The expression of annexin 1 was analyzed in more detail. At the RNA level, ANX1 expression was barely detectable in normal pancreatic tissues, and most of the cases of chronic pancreatitis showed only a slight increase in ANX1 expression, whereas in one case, the expression was markedly upregulated to levels comparable to the expression level detectable in pancreatic carcinoma (Figure 3). Comparable results were obtained at the protein level using immunohistochemistry. The staining pattern for ANX1 in CP ranged from samples with no obvious staining to samples with single nests of ANX1-positive ductal structures (Figure 4*A*) and samples in which the majority of the remaining exocrine tissues were ANX1-positive (Figure 4*C*); in one case, nuclear staining was also observable (Figure 4*B*). In ductal pancreatic adenocarcinoma, tumor cells stained positive (Figure 4*D*).

Discussion

In the last decades, knowledge concerning the molecular pathology of pancreatic ductal adenocarcinoma (PDAC) has

Table 3. Results of MALDI-TOF-MS and Database Search for Differentially Expressed Proteins in VAras^{mut} Cells.

Protein Name	Taxonomy*	Accession Number	Mascot Score†	Peptides Matched	Peptide Coverage (%)	Molecular Weight M_w (Theoretical/ Experimental; kDa)	p*I* (Theoretical/ Experimental)	VAras^{mut}/VA‡	± SD
Keratin type II, cytoskeletal 8	B	P05786	239	17	55	42.2/53.3	5.13/5.92	+ 3.3	± 0.3
Stress-induced phosphoprotein 1	M	AAH03794	102	10	20	63.2/64.6	6.40/6.27	+ 3.0	± 1.2
Heat shock 70-kDa protein 8	B	NP_776770	133	12	24	71.4/71.5	5.49/5.50	+ 2.8	± 0.9
Heat shock 27-kDa protein	C	P42929	92	7	30	22.9/25.0	6.23/6.11	+ 2.6	± 1.0
Heat shock 70-kDa protein 8 isoform	B	NP_776770	66	7	12	71.4/71.5	5.49/5.45	+ 2.3	± 0.2
Glucose-regulated protein 58 kDa	B	NP_776758	280	20	42	57.3/58.6	6.23/6.16	+ 2.1	± 0.4
Annexin 1	B	NP_786978	190	13	48	39.1/35.8	6.44/6.39	+ 1.9	± 1.4
Rho GDP dissociation inhibitor α	B	NP_788823	129	8	37	23.5/26.5	5.12/5.24	+ 1.8	± 0.5
β/γ Actin	M	CAA31455	95	8	26	41.3/44.1	5.56/5.43	+ 1.8	± 1.0
Heat shock 70-kDa protein 5	H	NP_005338	147	12	24	72.4/75.2	5.07/5.12	+ 1.6	± 0.2
β Tubulin [fragmented protein]	M	NP_076205	197	14	27	50.4/36.0	4.78/5.59	+ 1.6	± 0.6
γ Actin	H	AAA51580	81	5	21	26.1/26.1	5.65/5.65	− 1.6	± 0.7
α Tubulin [fragmented protein]	H	NP_116093	93	8	26	50.5/38.3	4.96/5.67	− 1.8	± 0.7
Tropomyosin 1	H	NP_000357	105	9	25	32.8/31.2	4.81/4.69	− 1.9	± 0.8
Keratin, type II cytoskeletal 8 [fragmented protein]	B	P05786	115	8	25	42.4/26.4	5.13/5.01	− 2.0	± 1.1
Vimentin	B	NP_776394	187	15	42	53.7/47.7	5.20/4.89	− 2.1	± 0.7
β/γ Actin	B	ATBOB	86	6	20	41.9/41.9	5.31/5.29	− 2.1	± 1.2
Vimentin	B	NP_776394	130	11	31	53.7/44.9	5.20/4.68	− 2.5	± 0.9
Myosin regulatory light chain	H	NP_006462	60	4	29	19.8/21.2	4.67/4.60	− 3.0	± 0.2
Proliferating cell nuclear antigen	M	NP_035175	89	6	26	29.1/32.7	4.66/4.60	− 5.0	± 0.9

p*I* = isoelectrical point; SD = standard deviation.
*C = *Canis familaris*; B = *Bos taurus*; H = *Homo sapiens*; M = *Mus musculus*.
†The mascot score is measured as −10*log(*P*), where *P* is the absolute probability that the observed match is a random event.
‡Fold change: (+) an increase in protein expression in VAras^{mut} cells; (−) a decrease in protein expression in VAras^{mut} cells.

increased markedly. However, this disease still remains an unresolved problem due to late diagnosis, low resectability, and the almost complete resistance to conventional radiotherapy/chemotherapy [10]. Several studies attempted to identify new diagnostic markers or new therapeutic targets for PDAC by gene expression microarray analysis of either bulk tissue [11,12] or microdissected pancreatic cancer tissue [13,14]. These studies have identified a multitude of differentially expressed genes in PDAC and have contributed to a better understanding of the aggressive behavior of PDAC. However, there is little overlap of identified genes among various gene expression studies. Thus, comparison of the results of several expression studies in PDAC revealed that 148 of 978 [15] and 64 of 568 [16] differentially expressed genes were identified in at least 2 of 10 studies analyzed. As discussed in the latter two publications, this low concordance may be due to type, histology, and number of samples used, or to different platforms and analysis procedures applied. Moreover, changes at the RNA level do not always correlate with protein expression [17]; therefore, in the last years, proteomic approaches have been used to identify

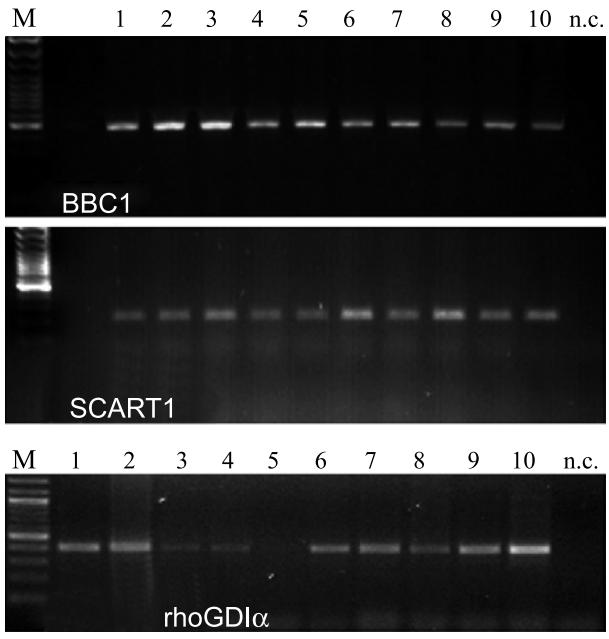

Figure 2. *Expression of the genes* BBC1, SCART1, *and* rhoGDIα *in normal pancreas (lanes 1–5) and pancreatic cancer (lanes 6–10), analyzed using semiquantitative RT-PCR.* BBC1 *was moderately downregulated and* rhoGDIα *was moderately upregulated, whereas for* SCART1, *no obvious change in expression level was detectable. The housekeeping gene* RPL13A *(lanes 1–5 and 11–15 in Figure 3 correspond to lanes 1–5 and 6–10 in this figure) was used for normalization. nc = negative control.*

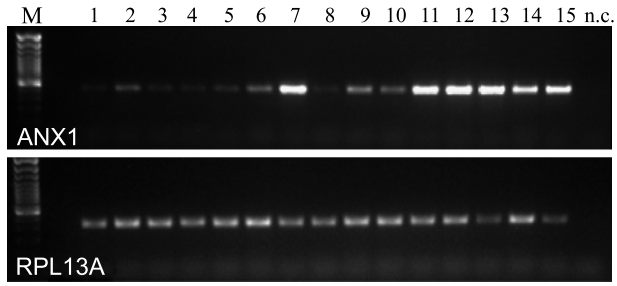

Figure 3. *Marked upregulation of annexin 1 expression in pancreatic carcinoma (lanes 11–15) compared to normal pancreas (lanes 1–5) and chronic pancreatitis (lanes 6–10), analyzed using semiquantitative RT-PCR. The housekeeping gene* RPL13A *was used for normalization. nc = negative control.*

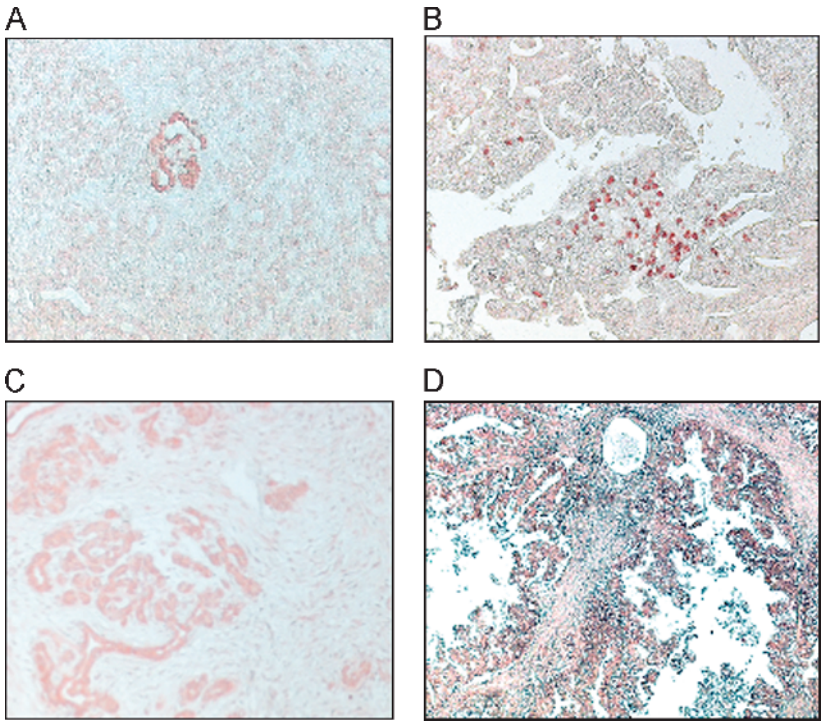

Figure 4. *Annexin 1 (ANX1) staining in chronic pancreatitis (A–C) and pancreatic adenocarcinoma (D). The staining pattern for ANX1 in CP ranged from single nests of ANX1-positive ductal structures (A) to samples in which the majority of the remaining exocrine tissues were ANX1-positive (C); in one case, nuclear staining was also observable (B). In pancreatic carcinoma, tumor cells stained positive (D).*

differentially expressed proteins in PDAC [18,19]. Taking the results of these proteomic approaches, only about 20% to 30% of differentially expressed proteins were reflected by concomitant changes at the mRNA level [20]. However, these studies, too, showed only little concordance of the results, probably due to the same factors already discussed for transcriptomic approaches.

Recently, we have demonstrated that the expression of a mutated *ki-ras* oncogene in immortalized pancreatic duct epithelial cells yielded a tumorigenic transformed phenotype [6]. Using this *in vitro* model of pancreatic carcinogenesis, we sought to overcome some of the problems described above. First, by the use of two cell lines differing only in the expression of a mutated *ki-ras*, a comparison of different cell types found in pancreatic cancer tissues was avoided. Moreover, our survey of ras transformation targets should augment the chance to identify marker molecules with expression changes early in the course of pancreatic carcinogenesis, as *ki-ras* mutations are detectable already in about 40% of PanIN-1 lesions associated with PDAC [5]. Comparable strategies were applied in two studies either by the inhibition of the expression of a mutated *ras* using antisense *k-ras*–transduced AsPC-1 cells [21] or by the expression of a mutated *k-ras* in HPV16-E6E7–immortalized human pancreatic duct epithelial cells [22]. Both studies analyzed differentially expressed genes at the RNA level. In the former study using the differential display technique, 20 differentially expressed genes were identified, of which > 50% were mitochondrial genes. In the latter study using Affymetrix gene chip arrays, about 1050 differentially expressed genes induced by the expression of the mutated *k-ras* gene were identified. However, only 5% of these genes have been reported previously as differentially expressed in PDAC or pancreatic tumor cell lines. To overcome these limitations, we combined transcriptomic and proteomic techniques in one study to identify targets with differential expressions both at the mRNA level and at the protein level. Using this approach, we identified 28 unique genes and 6 ESTs differentially expressed at the mRNA level using SSH analysis, and 15 unique differentially expressed proteins using 2D PAGE and MS analysis. In our study, as in others [17,20], concordance between mRNA and protein data was only marginal. Thus, only highly abundant proteins such as actin and CKs were identified by both techniques. This may be due to the lower dynamic range of the 2D PAGE protocol, which allows less abundant proteins to escape detection [23]. However, many of the differentially expressed molecules identified with either method (14 of 28 genes and 6 of 15 proteins; Tables 2 and 3) already had been demonstrated to be differentially expressed in pancreatic adenocarcinoma or to be influenced by a mutated *ras*, thus proving the validity of our model. To further validate our model, the expression of several genes was analyzed by RT-PCR and immunohistochemistry in samples from normal human pancreas, chronic pancreatitis, and PDAC. For three of four genes analyzed (*BBC1*, *rhoGDIα*, and *ANXA1*), the trend observed in our model system was also detectable in PDAC samples, again proving the validity of our model.

Due to the high number of differentially expressed genes and proteins, only a selected set of these molecules will be discussed in more detail. The majority of the expression changes identified affected cytoskeletal proteins. The cytoskeleton is involved in numerous cellular functions such as cell motility, mitogenesis, morphology, muscle contraction, cytokinesis, and establishment of cell polarity. Deregulated expression and reorganization of cytoskeletal proteins are associated with the development of various forms of cancer [24]. In our study, we found an overexpression at the RNA level of CKs such as CK7, CK8, and CK19, as well as of myosin regulatory light chain. Overexpression of these CKs already has been reported in pancreatic carcinoma in several other gene expression studies [11,12], and myosin regulatory light chain has been shown to be involved in the invasion and adhesion of pancreatic cancer cells [25]. At the protein level, the results concerning CK expression were quite different. Here only a translationally modified isoform of CK8 was detectable, showing an increased apparent molecular weight compared to the theoretical value, and this isoform was upregulated in VAras^{mut} cells.

A fragmented form of CK8 and additionally fragmented forms of the cytoskeletal proteins α tubulin, β tubulin, and vimentin were identified, which, except for β tubulin, were all downregulated in VAras^{mut} cells. Although we cannot rule out that the fragmentation of these proteins happened during the isolation of the proteins, the other proteins identified in this study were not fragmented, which argues against this possibility. Proteolytic degradation of several proteins, including nuclear lamins, CKs, and vimentin, is a hallmark of the dramatic cytoskeletal reorganization that occurs during apoptosis [26–28]. Caspase-mediated fragmentation of CK18 and CK19 during apoptosis generated stable fragments with a defined molecular weight (CK18: 29 and 23 kDa; CK19: 28 and 20 kDa), whereas type II CKs (e.g., CK8) are virtually resistant to this degradation [27]. Because CK8 fragments have been detected, caspase-mediated fragmentation appears not to be the cause of the observed CK degradation. However, the release of proteolytically processed CKs (CK8, CK18, and CK19) into the culture medium was reported for the mammary tumor cell line MCF-7 [29]. This release of fragmented CKs resulted in the development of serum tumor markers such as TPS (CK18 fragment) and CYFRA 21-1 (CK19 fragment) [30]. Although these markers traditionally have been considered as markers of tumor proliferation, more recently, it has been shown that these markers are also released during the apoptosis of epithelial tumor cells [31]. Therefore, the reduced level of CK8 fragmentation may be an indicator of a reduced basal apoptotic rate in VAras^{mut} cells.

The α and β tubulin fragments were slightly underrepresented and overrepresented in VAras^{mut} cells, respectively. In contrast, vimentin fragments were markedly decreased in VAras^{mut} cells. Like CKs, tubulin [32] and vimentin [33] are also cleaved during apoptosis. Caspase-mediated proteolysis of vimentin results in the generation of several fragments, including fragments of about 48 and 45 kDa [28], which were also identified in our study. Thus, the decreased fragmentation of α tubulin and vimentin again indicates a reduced basal rate of apoptosis in VAras^{mut} cells.

Another large group of proteins with altered expression consisted of HSPs and cochaperones. All of these proteins (HSP70, HSP27, Grp58, and stress-induced phosphoprotein 1, also called HSP70/HSP90 organizing protein/HOP) were upregulated in VAras^{mut} cells. HSPs were discovered as a group of proteins that are induced by various kinds of stress [34]; they facilitate the correct folding of other proteins under physiological and stress conditions with the help of cochaperones such as HOP [35]. Overexpressed HSP27 and HSP70 prevent the apoptosis induced by various stimuli, including hyperthermia, oxidative stress, CD95 ligation, or chemotherapy, by interfering with the action of key apoptotic proteins, such as Bid, Bax, apoptosis-inducing factor, and apoptosis protease–activating factor 1. Moreover, the signaling of survival factors through the PI3K/Akt pathway is promoted by the binding of HSP27 to Akt (reviewed in Garrido et al. [36]). HSPs are overexpressed in various forms of cancer, such as breast cancer [37], gastric cancer [38], colorectal carcinoma [39], and pancreatic carcinoma [40]. HSP27 and HSP70 expressions are associated with the invasion and metastasis of xenotransplanted human breast cancer cells [41] and with an increase in the tumorigenic potential of a mouse fibrosarcoma model [42], respectively. Increased HSP27 and HSP70 expression in acute myeloid leukemia, esophageal carcinomas, and colonic cancers has been associated with poor prognosis [43], resistance to radiotherapy and chemotherapy [44], and metastasis [45]. In contrast, pancreatic carcinoma patients with extensive HSP70 staining of tumor cells had a better prognosis [46]. In normal cells, the chaperone Grp58, a member of the protein disulfide isomerase family, is an integral part of the peptide-loading complex of the MHC class I molecules [47] and also is implicated in signaling by Stat3 [48]. Expression of Grp58 was induced in v-onc–transformed and v-src–transformed kidney cells and fibroblasts, respectively [49]. Additionally, overexpression of Grp58 was associated with chemoresistance in oral squamous cell carcinoma [50] and serous epithelial ovarian carcinoma [51]. However, inhibition of Grp58 expression by siRNA decreased mitomycin C–induced cytotoxicity in human colon carcinoma cells [52]. Thus, the increased expression of HSPs, HOP, and Grp58 observed in VAras^{mut} cells may confer an increased resistance to apoptosis in cells. The resulting reduced apoptotic rate could be reflected by the observed reduced fragmentation of cytoskeletal proteins, as discussed above.

Two putative tumor-suppressor genes, *GLTSCR2* and *BBC1*, were downregulated in ki-ras–transfected cells. Recently, the stabilization of the tumor-suppressor PTEN by the protein PICT-1, encoded by *GLTSCR2*, was demonstrated in human breast cancer MCF-7 cells [53]. Thus, the reduced expression of *GLTSCR2* may explain the loss of PTEN observable in pancreatic cancer cells without concomitant mutation or promoter methylation of the *PTEN* gene [54,55]. The gene *BBC1* located on chromosome 16 was originally described as a putative breast-tumor-suppressor gene [56]. Allelic loss of the chromosome region of *BBC1* (16q22–q24)

was associated with sporadic breast cancer [57]. However, in a later study, no tumor-specific mutations in the *BBC1* gene were detected in a selected set of breast tumors that showed loss of heterozygosity (LOH) at 16q24, thus excluding *BBC1* as a candidate breast-tumor-suppressor gene [58]. Also in prostate cancer, several studies demonstrated LOH of the *BBC1* region in prostatic cancer [59,60], which increased in higher-grade tumors and metastases. Up to now, only one publication has reported a loss of the chromosomal region of *BBC1* (16q22–q24) in pancreatic cancer [61], and in our small series of five pancreatic adenocarcinoma samples, a clear trend toward a reduced *BBC1* expression was detectable, encouraging further studies on *BBC1* as a tumor-suppressor gene in PDAC.

rhoGDIα is a cellular regulatory protein that acts primarily by controlling the cellular distribution and activity of rho GTPases [62], which transduce external signals to multiple downstream targets to elicit a variety of cellular responses such as organization of the actin cytoskeleton, cell cycle progression, cell polarity, and morphology [63]. GDIs typically act as negative regulators of rho GTPases through inhibition of GDP–GTP exchange [64]. Nevertheless, it has been demonstrated that rhoGDI, despite being a negative regulator of Cdc42 activation, is required for Cdc42-mediated cellular transformation [65]. Moreover, rhoGDI is overexpressed in a variety of cancers such as ovarian cancer [66], breast cancer [67], and lung cancer [68]. To our knowledge, except for the present study, there is only one additional publication concerning the overexpression of *rhoGDIα* in PDAC [69]. Additionally, rhoGDI overexpression is associated with chemoresistance in ovarian cancer [70], breast cancer [71], and melanoma [72]. Given the almost complete resistance of PDAC to conventional chemotherapy, the role of *rhoGDIα* overexpresson in pancreatic cancer warrants further analysis.

The protein annexin 1 was found to be overexpressed in $VAras^{mut}$ cells. Annexin 1, also called lipocortin 1, belongs to a large family of Ca^{2+}-dependent phospholipid-binding proteins [73]. It is a glucocorticoid-regulated protein and shares many anti-inflammatory effects with these drugs, such as inhibition of cell proliferation, regulation of cell migration, and apoptosis [74,75]. Overexpression of annexin 1 has been reported for various cancers such as breast cancer [76] and hepatocellular carcinoma [77]. However, its downregulation was found, for example, in esophageal and prostate carcinoma [78]. In pancreatic carcinoma, overexpression of annexin 1 was demonstrated at the RNA level [12,14] and at the protein level [19] and correlated with a poorly differentiated phenotype of tumor cells [79]. Increased annexin 1 expression was demonstrated in drug-resistant tumor cells of the stomach [80], prostate [81], and breast [82]. Thus, the overexpression of annexin 1 may be responsible, at least in part, for the chemoresistance found in virtually all pancreatic carcinomas.

In conclusion, we have demonstrated that the transfection of a mutated *ki-ras* was accompanied by a specific expression pattern of several genes and proteins, which may result in an increase in malignant potential and an increased resistance to the apoptosis of transfected $VAras^{mut}$ cells. Thus, our *in vitro* model is a valuable tool that may be used to analyze the role of genetic alterations implicated in the early stages of tumor development in PDAC. The combination of two different approaches studying gene expression, namely, transcriptomics and proteomics, allowed for the identification of potential targets for the early diagnosis and/or therapy of pancreatic carcinoma, whereas these targets would have been missed by using only one of these two techniques.

Acknowledgements

We would like to thank Swelana Sander-Naderi, Sarina Löffler, and Anette Funk for technical assistance, and Wolfgang Hagmann for critical review of the manuscript.

References

[1] Jemal A, Siegel R, Ward E, Murray T, Xu J, Smigal C, and Thun MJ (2006). Cancer statistics, 2006. *CA Cancer J Clin* **56**, 106–130.

[2] Freelove R and Walling AD (2006). Pancreatic cancer: diagnosis and management. *Am Fam Phys* **73**, 485–492.

[3] Morohoshi T, Held G, and Klöppel G (1983). Exocrine pancreatic tumours and their histological classification. A study based on 167 autopsy and 97 surgical cases. *Histopathology* **7**, 645–661.

[4] Grapin-Botton A (2005). Ductal cells of the pancreas. *Int J Biochem Cell Biol* **37**, 504–510.

[5] Löhr M, Klöppel G, Maisonneuve P, Lowenfels AB, and Lüttges J (2005). Frequency of *K-ras* mutations in pancreatic intraductal neoplasias associated with pancreatic ductal adenocarcinoma and chronic pancreatitis: a meta-analysis. *Neoplasia* **7**, 17–23.

[6] Löhr M, Müller P, Zauner I, Schmidt C, Trautmann B, Thevenod F, Capella G, Farre A, Liebe S, and Jesnowski R (2001). Immortalized bovine pancreatic duct cells become tumorigenic after transfection with mutant *k-ras*. *Virchows Arch* **438**, 581–590.

[7] Diehl F, Grahlmann S, Beier M, and Hoheisel JD (2001). Manufacturing DNA microarrays of high spot homogeneity and reduced background signal. *Nucleic Acids Res* **29**, E38.

[8] Fielden MR, Halgren RG, Dere E, and Zacharewski TR (2002). GP3: GenePix post-processing program for automated analysis of raw microarray data. *Bioinformatics* **18**, 771–773.

[9] Mortz E, Krogh TN, Vorum H, and Gorg A (2001). Improved silver staining protocols for high sensitivity protein identification using matrix-assisted laser desorption/ionization–time of flight analysis. *Proteomics* **1**, 1359–1363.

[10] Bardeesy N and DePinho RA (2002). Pancreatic cancer biology and genetics. *Nat Rev Cancer* **2**, 897–909.

[11] Friess H, Ding J, Kleeff J, Fenkell L, Rosinski JA, Guweidhi A, Reidhaar-Olson JF, Korc M, Hammer J, and Büchler MW (2003). Microarray-based identification of differentially expressed growth- and metastasis-associated genes in pancreatic cancer. *Cell Mol Life Sci* **60**, 1180–1199.

[12] Iacobuzio-Donahue CA and Hruban RH (2003). Gene expression in neoplasms of the pancreas: applications to diagnostic pathology. *Adv Anat Pathol* **10**, 125–134.

[13] Crnogorac-Jurcevic T, Efthimiou E, Nielsen T, Loader J, Terris B, Stamp G, Baron A, Scarpa A, and Lemoine NR (2002). Expression profiling of microdissected pancreatic adenocarcinomas. *Oncogene* **21**, 4587–4594.

[14] Grützmann R, Foerder M, Alldinger I, Staub E, Brummendorf T, Ropcke S, Li X, Kristiansen G, Jesnowski R, Sipos B, et al. (2003). Gene expression profiles of microdissected pancreatic ductal adenocarcinoma. *Virchows Arch* **443**, 508–517.

[15] Brandt R, Grützmann R, Bauer A, Jesnowski R, Ringel J, Löhr M, Pilarsky C, and Hoheisel JD (2004). DNA microarray analysis of pancreatic malignancies. *Pancreatology* **4**, 587–597.

[16] Grützmann R, Boriss H, Ammerpohl O, Lüttges J, Kalthoff H, Schackert HK, Klöppel G, Saeger HD, and Pilarsky C (2005). Meta-analysis of microarray data on pancreatic cancer defines a set of commonly dysregulated genes. *Oncogene* **24**, 5079–5088.

[17] Gygi SP, Rochon Y, Franza BR, and Aebersold R (1999). Correlation

between protein and mRNA abundance in yeast. *Mol Cell Biol* **19**, 1720–1730.

[18] Chen R, Yi EC, Donohoe S, Pan S, Eng J, Cooke K, Crispin DA, Lane Z, Goodlett DR, Bronner MP, et al. (2005). Pancreatic cancer proteome: the proteins that underlie invasion, metastasis, and immunologic escape. *Gastroenterology* **129**, 1187–1197.

[19] Crnogorac-Jurcevic T, Gangeswaran R, Bhakta V, Capurso G, Lattimore S, Akada M, Sunamura M, Prime W, Campbell F, Brentnall TA, et al. (2005). Proteomic analysis of chronic pancreatitis and pancreatic adenocarcinoma. *Gastroenterology* **129**, 1454–1463.

[20] Löhr JM, Faissner R, Findeisen P, and Neumaier M (2006). Proteome analysis—basis for individualized pancreatic carcinoma therapy? *Internist (Berlin)* **47** (1), S40–S48.

[21] Ohnami S, Matsumoto N, Nakano M, Aoki K, Nagasaki K, Sugimura T, Terada M, and Yoshida T (1999). Identification of genes showing differential expression in antisense K-ras–transduced pancreatic cancer cells with suppressed tumorigenicity. *Cancer Res* **59**, 5565–5571.

[22] Qian J, Niu J, Li M, Chiao PJ, and Tsao MS (2005). *In vitro* modeling of human pancreatic duct epithelial cell transformation defines gene expression changes induced by K-ras oncogenic activation in pancreatic carcinogenesis. *Cancer Res* **65**, 5045–5053.

[23] Shen J, Person MD, Zhu J, Abbruzzese JL, and Li D (2004). Protein expression profiles in pancreatic adenocarcinoma compared with normal pancreatic tissue and tissue affected by pancreatitis as detected by two-dimensional gel electrophoresis and mass spectrometry. *Cancer Res* **64**, 9018–9026.

[24] Yamazaki D, Kurisu S, and Takenawa T (2005). Regulation of cancer cell motility through actin reorganization. *Cancer Sci* **96**, 379–386.

[25] Kaneko K, Satoh K, Masamune A, Satoh A, and Shimosegawa T (2002). Myosin light chain kinase inhibitors can block invasion and adhesion of human pancreatic cancer cell lines. *Pancreas* **24**, 34–41.

[26] Rao L, Perez D, and White E (1996). Lamin proteolysis facilitates nuclear events during apoptosis. *J Cell Biol* **135**, 1441–1455.

[27] Ku NO, Liao J, and Omary MB (1997). Apoptosis generates stable fragments of human type I keratins. *J Biol Chem* **272**, 33197–33203.

[28] Byun Y, Chen F, Chang R, Trivedi M, Green KJ, and Cryns VL (2001). Caspase cleavage of vimentin disrupts intermediate filaments and promotes apoptosis. *Cell Death Differ* **8**, 443–450.

[29] Chan R, Rossitto PV, Edwards BF, and Cardiff RD (1986). Presence of proteolytically processed keratins in the culture medium of MCF-7 cells. *Cancer Res* **46**, 6353–6359.

[30] Pujol JL, Grenier J, Daures JP, Daver A, Pujol H, and Michel FB (1993). Serum fragment of cytokeratin subunit 19 measured by CYFRA 21-1 immunoradiometric assay as a marker of lung cancer. *Cancer Res* **53**, 61–66.

[31] Sheard MA, Vojtesek B, Simickova M, and Valik D (2002). Release of cytokeratin-18 and -19 fragments (TPS and CYFRA 21-1) into the extracellular space during apoptosis. *J Cell Biochem* **85**, 670–677.

[32] Asumendi A, Andollo N, Boyano MD, Hilario E, Perez-Yarza G, Atencia R, Arechaga J, and Garcia-Sanz M (2000). The role of cleavage of cell structures during apoptosis. *Cell Mol Biol (Noisy-le-Grand)* **46**, 1–11.

[33] Lavastre V, Chiasson S, Cavalli H, and Girard D (2005). Viscum album agglutinin-I induces apoptosis and degradation of cytoskeletal proteins *via* caspases in human leukaemia eosinophil AML14.3D10 cells: differences with purified human eosinophils. *Br J Haematol* **130**, 527–535.

[34] Lindquist S and Craig EA (1988). The heat-shock proteins. *Annu Rev Genet* **22**, 631–677.

[35] Odunuga OO, Longshaw VM, and Blatch GL (2004). Hop: more than an Hsp70/Hsp90 adaptor protein. *Bioessays* **26**, 1058–1068.

[36] Garrido C, Brunet M, Didelot C, Zermati Y, Schmitt E, and Kroemer G (2006). Heat shock proteins 27 and 70: anti-apoptotic proteins with tumorigenic properties. *Cell Cycle* **5**, 2592–2601.

[37] Tauchi K, Tsutsumi Y, Hori S, Yoshimura S, Osamura RY, and Watanabe K (1991). Expression of heat shock protein 70 and c-myc protein in human breast cancer: an immunohistochemical study. *Jpn J Clin Oncol* **21**, 256–263.

[38] Liu X, Ye L, Wang J, and Fan D (1999). Expression of heat shock protein 90 beta in human gastric cancer tissue and SGC7901/VCR of MDR-type gastric cancer cell line. *Chin Med J (Engl)* **112**, 1133–1137.

[39] Kanazawa Y, Isomoto H, Oka M, Yano Y, Soda H, Shikuwa S, Takeshima F, Omagari K, Mizuta Y, Murase K, et al. (2003). Expression of heat shock protein (Hsp) 70 and Hsp 40 in colorectal cancer. *Med Oncol* **20**, 157–164.

[40] Ogata M, Naito Z, Tanaka S, Moriyama Y, and Asano G (2000). Overexpression and localization of heat shock proteins mRNA in pancreatic carcinoma. *J Nippon Med Sch* **67**, 177–185.

[41] Lemieux P, Oesterreich S, Lawrence JA, Steeg PS, Hilsenbeck SG, Harvey JM, and Fuqua SA (1997). The small heat shock protein hsp27 increases invasiveness but decreases motility of breast cancer cells. *Invasion Metastasis* **17**, 113–123.

[42] Jaattela M (1995). Over-expression of hsp70 confers tumorigenicity to mouse fibrosarcoma cells. *Int J Cancer* **60**, 689–693.

[43] Steiner K, Graf M, Hecht K, Reif S, Rossbacher L, Pfister K, Kolb HJ, Schmetzer HM, and Multhoff G (2006). High HSP70-membrane expression on leukemic cells from patients with acute myeloid leukemia is associated with a worse prognosis. *Leukemia* **20**, 2076–2079.

[44] Miyazaki T, Kato H, Faried A, Sohda M, Nakajima M, Fukai Y, Masuda N, Manda R, Fukuchi M, Ojima H, et al. (2005). Predictors of response to chemo-radiotherapy and radiotherapy for esophageal squamous cell carcinoma. *Anticancer Res* **25**, 2749–2755.

[45] Wang XP, Qiu FR, Liu GZ, and Chen RF (2005). Correlation between clinicopathology and expression of heat shock protein 70 and glucose-regulated protein 94 in human colonic adenocarcinoma. *World J Gastroenterol* **11**, 1056–1059.

[46] Sagol O, Tuna B, Coker A, Karademir S, Obuz F, Astarcioglu H, Kupelioglu A, Astarcioglu I, and Topalak O (2002). Immunohistochemical detection of pS2 protein and heat shock protein-70 in pancreatic adenocarcinomas. Relationship with disease extent and patient survival. *Pathol Res Pract* **198**, 77–84.

[47] Antoniou AN, Ford S, Alphey M, Osborne A, Elliott T, and Powis SJ (2002). The oxidoreductase ERp57 efficiently reduces partially folded in preference to fully folded MHC class I molecules. *EMBO J* **21**, 2655–2663.

[48] Yu X, Guo ZS, Marcu MG, Neckers L, Nguyen DM, Chen GA, and Schrump DS (2002). Modulation of p53, ErbB1, ErbB2, and Raf-1 expression in lung cancer cells by depsipeptide FR901228. *J Natl Cancer Inst* **94**, 504–513 (April 3).

[49] Hirano N, Shibasaki F, Sakai R, Tanaka T, Nishida J, Yazaki Y, Takenawa T, and Hirai H (1995). Molecular cloning of the human glucose-regulated protein ERp57/GRP58, a thiol-dependent reductase. Identification of its secretory form and inducible expression by the oncogenic transformation. *Eur J Biochem* **234**, 336–342.

[50] Nakatani K, Nakamura M, Uzawa K, Wada T, Seki N, Tanzawa H, and Fujita S (2005). Establishment and gene analysis of a cisplatin-resistant cell line, Sa-3R, derived from oral squamous cell carcinoma. *Oncol Rep* **13**, 709–714.

[51] Bernardini M, Lee CH, Beheshti B, Prasad M, Albert M, Marrano P, Begley H, Shaw P, Covens A, Murphy J, et al. (2005). High-resolution mapping of genomic imbalance and identification of gene expression profiles associated with differential chemotherapy response in serous epithelial ovarian cancer. *Neoplasia* **7**, 603–613.

[52] Su S, Adikesavan AK, and Jaiswal AK (2006). si RNA inhibition of GRP58 associated with decrease in mitomycin C–induced DNA cross-linking and cytotoxicity. *Chem Biol Interact* **162**, 81–87.

[53] Okahara F, Ikawa H, Kanaho Y, and Maehama T (2004). Regulation of PTEN phosphorylation and stability by a tumor suppressor candidate protein. *J Biol Chem* **279**, 45300–45303.

[54] Okami K, Wu L, Riggins G, Cairns P, Goggins M, Evron E, Halachmi N, Ahrendt SA, Reed AL, Hilgers W, et al. (1998). Analysis of PTEN/MMAC1 alterations in aerodigestive tract tumors. *Cancer Res* **58**, 509–511.

[55] Asano T, Yao Y, Zhu J, Li D, Abbruzzese JL, and Reddy SA (2004). The PI 3-kinase/Akt signaling pathway is activated due to aberrant Pten expression and targets transcription factors NF-kappaB and c-Myc in pancreatic cancer cells. *Oncogene* **23**, 8571–8580.

[56] Adams SM, Helps NR, Sharp MG, Brammar WJ, Walker RA, and Varley JM (1992). Isolation and characterization of a novel gene with differential expression in benign and malignant human breast tumours. *Hum Mol Genet* **1**, 91–96.

[57] Schmutzler RK, Fimmers R, Bierhoff E, Lohmar B, Homann A, Speiser P, Kubista E, Jaeger K, Krebs D, Zeillinger R, et al. (1996). Association of allelic losses on human chromosomal arms 11Q and 16Q in sporadic breast cancer. *Int J Cancer* **69**, 307–311.

[58] Moerland E, Breuning MH, Cornelisse CJ, and Cleton-Jansen AM (1997). Exclusion of *BBC1* and *CMAR* as candidate breast tumour-suppressor genes. *Br J Cancer* **76**, 1550–1553.

[59] Visakorpi T, Kallioniemi AH, Syvanen AC, Hyytinen ER, Karhu R, Tammela T, Isola JJ, and Kallioniemi OP (1995). Genetic changes in primary and recurrent prostate cancer by comparative genomic hybridization. *Cancer Res* **55**, 342–347.

[60] Hugel A and Wernert N (1999). Loss of heterozygosity (LOH), malignancy grade and clonality in microdissected prostate cancer. *Br J Cancer* **79**, 551–557.

[61] Chang MC, Chang YT, Tien YW, Sun CT, Wu MS, and Lin JT (2005). Distinct chromosomal aberrations of ampulla of Vater and pancreatic

head cancers detected by laser capture microdissection and comparative genomic hybridization. *Oncol Rep* **14**, 867–872.
[62] Olofsson B (1999). Rho guanine dissociation inhibitors: pivotal molecules in cellular signalling. *Cell Signal* **11**, 545–554.
[63] Erickson JW and Cerione RA (2001). Multiple roles for Cdc42 in cell regulation. *Curr Opin Cell Biol* **13**, 153–157.
[64] Fukumoto Y, Kaibuchi K, Hori Y, Fujioka H, Araki S, Ueda T, Kikuchi A, and Takai Y (1990). Molecular cloning and characterization of a novel type of regulatory protein (GDI) for the rho proteins, ras p21–like small GTP-binding proteins. *Oncogene* **5**, 1321–1328.
[65] Lin Q, Fuji RN, Yang W, and Cerione RA (2003). RhoGDI is required for Cdc42-mediated cellular transformation. *Curr Biol* **13**, 1469–1479.
[66] Jones MB, Krutzsch H, Shu H, Zhao Y, Liotta LA, Kohn EC, Petricoin EF III (2002). Proteomic analysis and identification of new biomarkers and therapeutic targets for invasive ovarian cancer. *Proteomics* **2**, 76–84.
[67] Fritz G, Brachetti C, Bahlmann F, Schmidt M, and Kaina B (2002). Rho GTPases in human breast tumours: expression and mutation analyses and correlation with clinical parameters. *Br J Cancer* **87**, 635–644.
[68] MacKeigan JP, Clements CM, Lich JD, Pope RM, Hod Y, and Ting JP (2003). Proteomic profiling drug-induced apoptosis in non–small cell lung carcinoma: identification of RS/DJ-1 and RhoGDIalpha. *Cancer Res* **63**, 6928–6934.
[69] Lu Z, Hu L, Evers S, Chen J, and Shen Y (2004). Differential expression profiling of human pancreatic adenocarcinoma and healthy pancreatic tissue. *Proteomics* **4**, 3975–3988.
[70] Goto T, Takano M, Sakamoto M, Kondo A, Hirata J, Kita T, Tsuda H, Tenjin Y, and Kikuchi Y (2006). Gene expression profiles with cDNA microarray reveal RhoGDI as a predictive marker for paclitaxel resistance in ovarian cancers. *Oncol Rep* **15**, 1265–1271.
[71] Zhang B, Zhang Y, Dagher MC, and Shacter E (2005). Rho GDP dissociation inhibitor protects cancer cells against drug-induced apoptosis. *Cancer Res* **65**, 6054–6062.
[72] Poland J, Sinha P, Siegert A, Schnolzer M, Korf U, and Hauptmann S (2002). Comparison of protein expression profiles between monolayer and spheroid cell culture of HT-29 cells revealed fragmentation of CK18 in three-dimensional cell culture. *Electrophoresis* **23**, 1174–1184.
[73] Raynal P and Pollard HB (1994). Annexins: the problem of assessing the biological role for a gene family of multifunctional calcium- and phospholipid-binding proteins. *Biochim Biophys Acta* **1197**, 63–93.
[74] Kamal AM, Flower RJ, and Perretti M (2005). An overview of the effects of annexin 1 on cells involved in the inflammatory process. *Mem Inst Oswaldo Cruz* **100** (1), 39–47.
[75] Perretti M and D'Acquisto F (2006). Novel aspects of annexin 1 and glucocorticoid biology: intersection with nitric oxide and the lipoxin receptor. *Curr Drug Targets (Inflamm Allergy)* **5**, 107–114.
[76] Ahn SH, Sawada H, Ro JY, and Nicolson GL (1997). Differential expression of annexin I in human mammary ductal epithelial cells in normal and benign and malignant breast tissues. *Clin Exp Metastasis* **15**, 151–156.
[77] Masaki T, Tokuda M, Ohnishi M, Watanabe S, Fujimura T, Miyamoto K, Itano T, Matsui H, Arima K, Shirai M, et al. (1996). Enhanced expression of the protein kinase substrate annexin in human hepatocellular carcinoma. *Hepatology* **24**, 72–81.
[78] Paweletz CP, Ornstein DK, Roth MJ, Bichsel VE, Gillespie JW, Calvert VS, Vocke CD, Hewitt SM, Duray PH, Herring J, et al. (2000). Loss of annexin 1 correlates with early onset of tumorigenesis in esophageal and prostate carcinoma. *Cancer Res* **60**, 6293–6297.
[79] Bai XF, Ni XG, Zhao P, Liu SM, Wang HX, Guo B, Zhou LP, Liu F, Zhang JS, Wang K, et al. (2004). Overexpression of annexin 1 in pancreatic cancer and its clinical significance. *World J Gastroenterol* **10**, 1466–1470.
[80] Sinha P, Hutter G, Kottgen E, Dietel M, Schadendorf D, and Lage H (1998). Increased expression of annexin I and thioredoxin detected by two-dimensional gel electrophoresis of drug resistant human stomach cancer cells. *J Biochem Biophys Methods* **37**, 105–116.
[81] Carollo M, Parente L, and D'Alessandro N (1998). Dexamethasone-induced cytotoxic activity and drug resistance effects in androgen-independent prostate tumor PC-3 cells are mediated by lipocortin 1. *Oncol Res* **10**, 245–254.
[82] Wang Y, Serfass L, Roy MO, Wong J, Bonneau AM, and Georges E (2004). Annexin-I expression modulates drug resistance in tumor cells. *Biochem Biophys Res Commun* **314**, 565–570.

Table W1. All Identified Proteins in VAras^{mut} Cells and Their Fold Changes According to Four Biologic Replicates.

Protein Name	Taxonomy*	Accession Number	Molecular Weight M_w (Theoretical/Experimental; kDa)	pI (Theoretical/ Experimental)	SQ† 1		VAras^{mut}/VA‡			
					VAras^{mut}	VA	1	2	3	4
α Tubulin [fragmented protein]	H	NP_116093	50.5/38.3	4.96/5.67	4,485 ± 1,278	7,969 ± 4,917	− 1.80	− 1.50	− 2.80	+ 1.10
Annexin 1	B	NP_786978	39.1/35.8	6.44/6.39	14,871 ± 4,888	3,886 ± 1,802	+ 3.80	− 1.60	nd	+ 1.50
β/γ Actin	M	CAA31455	41.3/44.1	5.56/5.43	58,031 ± 13,449	27,218 ± 10,089	+ 2.10	− 1.15	+ 3.30	− 1.05
	M	CAA27396	39.1/38.2	5.78/5.69	3,342 ± 1,302	5,461 ± 4,311	− 1.60	nd	nd	+ 1.70
	B	ATBOB	41.9/41.9	5.31/5.29	2,525 ± 779	7,010 ± 2,339	− 2.80	+ 1.05	− 3.70	+ 1.10
	B	ATBOB	41.9/41.9	5.31/5.33	1,503 ± 522	3,497 ± 1,410	− 2.35	+ 1.30	− 1.55	+ 1.30
β Tubulin [fragmented protein]	M	NP_076205	50.4/36.0	4.78/5.59	7,512 ± 2,454	2,904 ± 2,238	+ 2.60	+ 1.30	+ 1.05	+ 1.40
Enolase 1	B	NP_776474	47.6/47.3	6.44/6.30	16,811 ± 7,415	1,107 ± 150	+ 15.20	− 1.75	nd	− 1.30
	B	NP_776474	47.6/47.7	6.44/6.15	5,717 ± 2,818	687 ± 292	+ 8.30	− 1.30	nd	±1.00
	B	NP_776474	47.6/47.3	6.44/6.44	25,349 ± 19,299	5,456 ± 3,847	+ 4.65	− 1.20	nd	nd
γ Actin	H	AAA51580	26.1/26.1	5.65/5.65	2,362 ± 1,133	6,581 ± 1,671	− 2.80	− 1.20	− 1.40	− 1.10
Glucose-regulated protein 58 kDa	B	NP_776758	57.3/58.6	6.23/6.16	17,627 ± 4,608	8,250 ± 4,153	+ 2.15	+ 1.35	+ 2.30	+ 2.40
Heat shock 27-kDa protein	C	P42929	22.9/25.0	6.23/6.11	20,923 ± 6,778	11,788 ± 4,010	+ 1.80	+ 4.40	+ 2.15	+ 2.05
Heat shock 70-kDa protein 5	H	NP_005338	72.4/75.2	5.07/5.12	7,416 ± 1,643	3,995 ± 2,135	+ 1.85	+ 1.45	+ 1.40	+ 1.80
Heat shock 70-kDa protein 8	B	NP_776770	71.4/71.5	5.49/5.50	23,658 ± 11,900	7,154 ± 3,899	+ 3.30	+ 1.70	+ 2.35	+ 4.00
	B	NP_776770	71.4/71.5	5.49/5.45	5,044 ± 2,138	2,061 ± 1,378	+ 2.45	+ 2.15	+ 2.40	nd
Keratin type I, cytoskeletal 19	B	P08728	43.9/41.7	4.92/5.02	11,770 ± 1,941	21,558 ± 17,399	− 1.80	+ 1.95	±1.00	+ 2.40
	B	P08728	43.9/39.1	4.92/4.73	486 ± 254	2,611 ± 445	− 5.40	nd	nd	nd
Keratin type II, cytoskeletal 8	B	P05786	42.2/53.3	5.13/5.92	11,109 ± 1,853	3,051 ± 2,970	+ 3.65	+ 2.90	nd	+ 3.20
	B	P05786	42.4/48.7	5.13/5.65	517 ± 234	2,984 ± 1,333	− 5.75	nd	nd	nd
Keratin, type II cytoskeletal 8 [fragmented protein]	B	P05786	42.4/26.4	5.13/5.01	1,698 ± 730	3,698 ± 1,173	− 2.15	− 2.65	− 3.00	+ 2.00
	B	P05786	42.4/25.0	5.13/4.60	4,605 ± 1,768	8,745 ± 3,563	− 1.90	+ 1.30	+ 1.40	+ 1.75
Myosin regulatory light chain	H	NP_006462	19.8/21.2	4.67/4.60	1,237 ± 1,043	3,481 ± 2,016	− 2.80	nd	− 3.25	nd
N-acetyl-galactosaminyl-transferase			/37.6	/6.25	1,305 ± 650	1,746 ± 490	− 1.35	+ 1.10	±1.00	+ 1.80
Peroxyredoxin 2	B	NP_777188	22.2/23.7	5.37/5.37	8,364 ± 2,228	6,889 ± 1,767	+ 1.20	+ 1.10	− 1.20	+ 1.10
Proliferating cell nuclear antigen	M	NP_035175	29.1/32.7	4.66/4.60	583 ± 155	2,360 ± 922	− 4.05	− 4.80	− 6.20	nd
RhoGDP dissociation inhibitor α	B	NP_788823	23.5/26.5	5.12/5.24	4,143 ± 1,399	1,710 ± 441	+ 2.40	nd	+ 1.90	+ 1.20
Stress-induced phosphoprotein 1	M	AAH03794	63.2/64.6	6.40/6.27	8,770 ± 2,853	1,916 ± 1,324	+ 4.60	+ 2.20	+ 3.65	+ 1.60
Triosephosphate isomerase 1	H	NP_000356	26.9/25.5	6.45/6.38	5,515 ± 1,647	2,678 ± 1,452	+ 2.05	− 1.90	nd	nd
Tropomyosin 1	H	NP_000357	32.8/31.2	4.81/4.69	2,591 ± 2,002	8,033 ± 3,534	− 3.10	− 1.60	+ 1.25	− 2.10
Tropomyosin 4	H	NP_003281	28.6/28.6	4.67/4.75	3,153 ± 732	2,178 ± 1,746	+ 1.45	− 1.15	+ 1.80	nd
Tropomyosin 5	M	S11390	29.2/28.6	4.75/4.80	16,990 ± 3,996	10,520 ± 2,250	+ 1.60	±1.00	+ 1.10	− 1.40
Tropomyosin 5	M	S11390	29.2/28.6	4.75/4.67	16,548 ± 3,928	24,044 ± 10,393	− 1.45	+ 1.20	+ 1.60	+ 1.05
Vimentin	B	NP_776394	53.7/51.6	5.20/5.00	3,878 ± 5,754	5,479 ± 2,098	− 1.40	− 1.40	+ 2.10	− 1.90
	B	NP_776394	53.7/47.7	5.20/4.89	1,249 ± 619	3,774 ± 1,918	− 3.00	− 2.10	− 2.15	− 1.10
	B	NP_776394	53.7/44.9	5.20/4.68	1,371 ± 827	4,917 ± 1,818	− 3.60	− 2.25	− 1.55	nd

nd = not detected in gel or no quantitation possible.

*C = *C. familaris*; B = *B. taurus*; H = *H. sapiens*; M = *M. musculus*.

†SQ = mean spot quantity and standard deviation (technical replicates) of experiment 1; normalized by total quantity in valid spots. SQs of experiments 2 to 4 are not shown.

‡Fold change: (+) an increase in protein expression in VAras^{mut} cells; (−) a decrease in protein expression in VAras^{mut} cells.